atmosphere

MDPI

Communication

Charged Atmospheric Aerosols from Charged Saltating Dust Aggregates

F. Chioma Onyeagusi *, Christian Meyer, Jens Teiser, Tim Becker and Gerhard Wurm

Faculty of Physics, University of Duisburg-Essen, Lotharstr. 1, 47057 Duisburg, Germany
* Correspondence: florence.onyeagusi@uni-due.de

Abstract: Grain collisions in aeolian events, e.g., due to saltation, result in atmospheric aerosols. They may regularly be electrically charged, but individual charge balances in collisions including small grains are not easily obtained on the ground. We therefore approach this problem in terms of microgravity, which allows for the observation of collisions and the determination of small charges. In a drop tower experiment, ∼1 mm dust aggregates are traced before and after a collision within the electric field of a plate capacitor. The sum of the electric charge of two particles (total charge) before and after the collision often strongly deviates from charge conservation. Due to the average low collision velocities of 0.2 m/s, there is no large scale fragmentation. However, we do observe small charged particles emerging from collisions. The smallest of these particles are as small as the current resolution limit of the optical system, i.e., they are at least as small as tens of µm. In the given setting, these small fragments may carry 1 nC/m^2–1 µC/m^2, which is between 1 % and ten times the surface charge density of the large aggregates. These first experiments indicate that collisions of charged aggregates regularly shed charged grains into the atmosphere, likely down to the suspendable aerosol size.

Keywords: aeolian transport; saltation; fragmentation; dust physics; charged aerosols; charge transfer

Citation: Onyeagusi, F.C.; Meyer, C.; Teiser, J.; Becker, T.; Wurm, G. Charged Atmospheric Aerosols from Charged Saltating Dust Aggregates. *Atmosphere* **2023**, *14*, 1065. https://doi.org/10.3390/atmos14071065

Academic Editors: Mamadou Sow and Noureddine Zouzou

Received: 12 May 2023
Revised: 13 June 2023
Accepted: 17 June 2023
Published: 24 June 2023

1. Introduction

Dust particles which are small enough to become suspended in a planetary atmosphere are regularly emitted during aeolian events [1–4]. This holds for dust on Earth but also on other planets such as Mars. This may not be taken for granted as micrometer grains are rather adhesive. Nevertheless, Becker et al. [5] recently showed in detail that the release of particles even smaller than 1 µm from a dust bed is already possible in rather moderate collisions. The solid impactors were of the order from 100 to 200 µm and had impact speeds of only about 1 m/s. That work did not probe a wider parameter range, but it is likely that dust is regularly emitted in any collision of aggregates with small dust grains adhering to them. This is a premise of the work presented here and may especially be of relevance as the nature of impactors is often of an aggregated rather than monolithic kind [6].

As particles collide, tribocharging or collisional charging is an important process that can hardly be avoided [7–9]. Rather generally, significant parts of atmospheric electricity may originate from this. Most regularly, this can be observed in thunderstorms, wherein charge separation occurs in collisions between ice particles. On Mars, this is probably more related to the collisions of dry grains [10]. On Earth, volcanic eruptions are accompanied by intense lightning, which implies charge generation and separation [11]. Dust storms and lower-level events come with charge separation as well [10,12–14]. This should support lifting grains into the atmosphere [15]. As a matter of fact, Esposito et al. [16] found that these electric fields can strongly increase the amount of material lifted. Onyeagusi et al. [17] studied this additional lifting force in an electric field on an individual grain level in drop tower experiments. They showed that basalt dust aggregates, adhering

to a conductive surface in a strong electric field charge until the repulsive force is strong enough to outweigh adhesion.

We connect this work to the one by Onyeagusi et al. [17]; while the previous work looked into the charging behavior of dust aggregates on a conductive surface within an electric field, we now study the charge exchange during the collision of two such aggregates. We focus on the charge balance of these collisions. Naively, one may expect the total charge on two grains to be conserved as they are supposed to exchange charges only between one another. Tribocharging is regularly discussed with only the two contact surfaces in mind. However, grains or surfaces never charge infinitely. With a charge limit, e.g., due to atmospheric breakdown, it is likely, if not imperative, that the charge before and after a collision is not preserved. In fact, breakdown can occur on small particle size scales [18–20]. It was shown recently by Jungmann et al. [21], who studied collisions between spherical (sub-)mm size glass particles, that some charge can indeed be emitted into the gas phase during these collisions. Gas phase ions are interesting for atmospheric electricity but only serve as a motivation here to have a detailed look at charge balances. In the following, we investigate charge balances on basalt aggregates in addition to monolithic basalt particles. As mentioned before, dust will regularly be released in collisions of aggregates. Therefore, the charge balance will also include some charge going astray with ejected dust particles or aggregate fragments. If the grains are small enough, they can be entrained into the atmosphere and become charged aerosols. This is the assumption we will support with this work. The rationale and structure of this paper are as follows: We first describe the microgravity experiments. We will then discuss the charge balance on two different kinds of particles, namely solid basalt spheres which are not supposed to lose grains in a collision and basalt aggregates which may lose small fragments. For the latter, we give examples of small, charged particles being ejected and estimate their size and charge distributions. This way, we investigate the charging behavior and the small-scale fragmentation of particles and dust aggregates in view of electrostatic processes in aeolian events as well as the suspension of µm-grains into the atmosphere.

2. Materials and Methods

The microgravity experiments are conducted at the drop tower in Bremen. We use a sample consisting of monolithic 550 µm (diameter) basalt beads and mm-sized basaltic dust aggregates. The setup is launched and experiences 9 s of microgravity. The experiment setup is shown in Figure 1.

In preparation for the experiment, the sample is placed in the particle compartment, which is also coated with the sample material to avoid a charging bias. This way, there are only same particle collisions. Right before launch, the particle compartment, which is mounted on top of a voice coil, starts shaking in order to induce collisions between particles to charge the sample. As soon as the experiment is launched and microgravity sets in, the sample is injected into the chamber volume of $50 \times 50 \times 110\,\mathrm{mm}^3$ where it can move freely within an electric field of up to 160 kV/m which is applied between the two electrodes at the sides. The chamber is illuminated from behind. A camera records the experiment through the front window. In order to prevent the sample from sticking to the walls, a DC motor on top of the setup can induce vibrations in the whole structure. In this particular experiment, charged particles that are floating through the experiment chamber are accelerated by the DC voltage that is applied to the plate capacitor. As the constant acceleration a along the electric field E is solely driven by the Coulomb force, the charge q of a particle with the mass m can be derived by $ma = qE$. This gives

$$q = \frac{a\rho\pi d^3}{6E}, \tag{1}$$

where d is the diameter and ρ is the density of the particle. This way, we can calculate the charge of two particles before and after they collide. The particles are traced manually using the ImageJ distribution Fiji [22]. This gives the frame-by-frame x-y positions of the

individual grains. An overlay of an example collision is shown in Figure 2. Particles collide with average velocities of about 0.2 m/s.

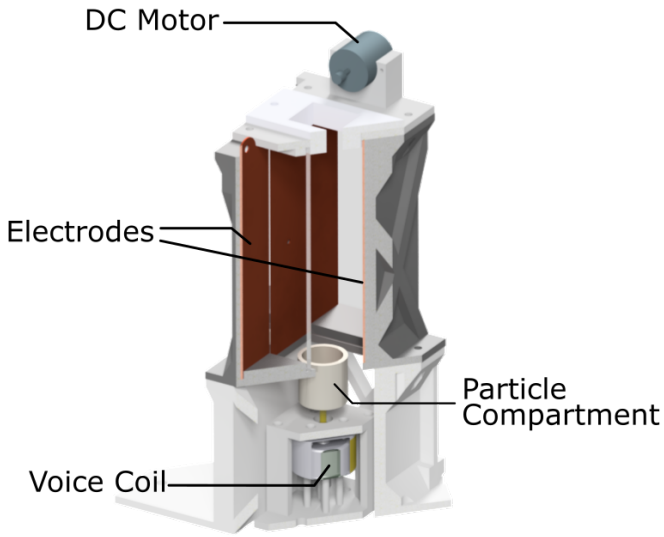

Figure 1. Schematics of the experiment setup. A voice coil shakes the particle compartment to electrically charge the sample. An electric field between the electrodes (plate capacitor) deflects the grains for charge measurements before and after collisions. Particle motion is observed by a camera (not shown). The DC motor can shake the whole chamber to release sticking grains from surfaces.

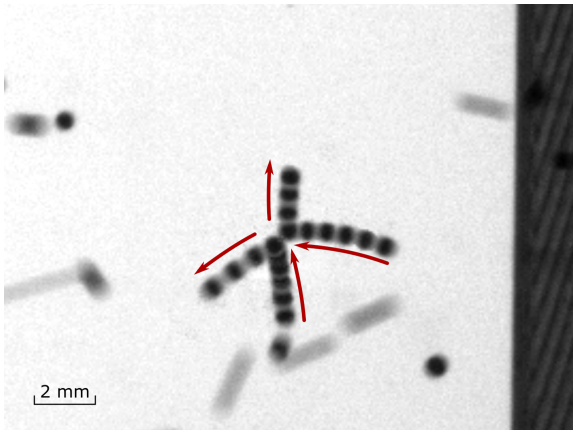

Figure 2. Example of a collision between two basalt beads. The trajectory of the beads is marked by the arrows. The particles are moving in microgravity; accelerations are caused by an electric field of 80 kV/m pointing upward.

3. Results and Discussion

We discuss two different particle samples here, sub-mm-sized spherical basalt beads and mm-sized aggregates consisting of µm basalt dust grains.

3.1. Collisions of Basalt Beads

First, we discuss collisions of commercial basalt beads (manufactured by Whitehouse Scientific), which are spherical and monolithic. A picture of these grains is shown in Figure 3.

We do not expect these grains to fragment during the vibrations that charge the grains as the respective collisions are rather moderate. We cannot completely rule out abrasion. However, if there is abrasion, it is so minimal that it is not visible within the resolution of the experiment. Therefore, any exchange of charge will be restricted to the two colliding grains and the surrounding gas. We cannot track charges within the gas with the given setup. What we can measure, however, is the total charge on two spheres before and after a collision. This is shown in Figure 4.

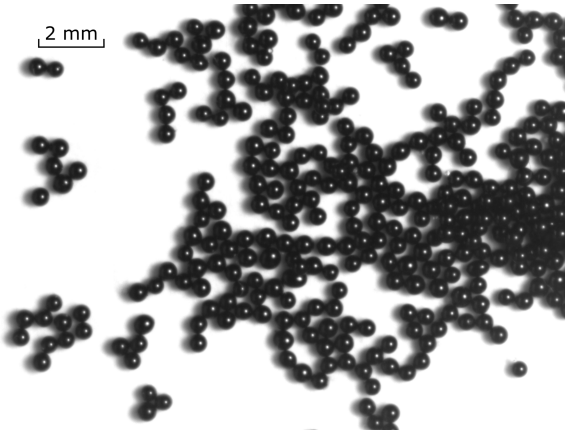

Figure 3. Basalt beads used as one sample. These solid sub-mm grains are not supposed to fragment in a slow collision.

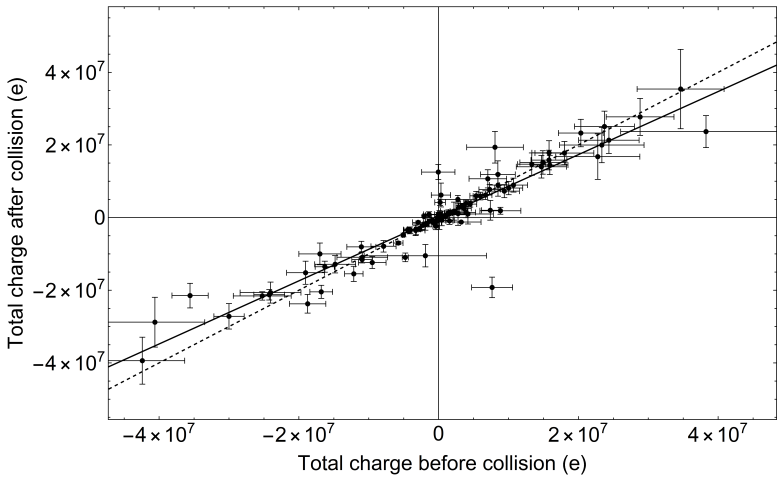

Figure 4. Total charge on two solid basalt spheres before and after a collision. The solid line is a linear approximation of the data. The dashed line visualizes charge conservation. The basalt bead systems tend to lose charge after a collision.

Most of the collisions are, individually, consistent with charge conservation, but there are some systematic deviations. Overall, there is a slight trend of two-particle systems losing charge. This trend is not as clear as in Jungmann et al. [21] for glass spheres. As collisions do not produce significant small grain fragments that may be ejected unnoticed, the small deviation from charge conservation is likely due to a fraction of the charge being transferred into the gas phase.

This can be the result of several processes. As the experiments were conducted at ambient pressure, it may be possible that discharge occurs over time through atmospheric ions. This kind of discharge over time should, however, be visible in the trajectories of the grains, expressed as a change in acceleration. As the accelerations that we measure are constant, we rule out atmospheric ions as the main cause for the observed discharge. Another possibility may be charge transfer during atmospheric breakdown. Breakdown can already be reached on small scales [18–20,23]. Here, electrons or ions can be transferred as charge carriers from the particles into the gas phase. Lastly, ions can be transferred directly from the particle surface into the surrounding gas. There are always a few layers of water adsorbed to the surface of our particles. Water ions are proposed to be a charge carrier during charge transfer between two colliding particles [24–26]. Therefore, water ions could not only be transferred from one particle to another, but they could also be suspended into the surrounding gas. In any case, the fraction of charge that we observe to be transmitted into the atmosphere is not large enough for this particular sample.

3.2. Collisions of Basalt Dust Aggregates

Based on the results for spherical grains, we would not expect much charge to be transferred into the gas phase from dust aggregates either. The aggregates were prepared in the laboratory. As base material we used basalt grains. The basalt is composed mainly of silicates and metal oxides. The original sample has a grain size of $\leq$200 µm and was milled with a planetary ball mill (PM 100 CM) into finer dust with an average particle size of a few µm. Afterward, those fine grains were vibrated to create the aggregates through sticking and compacting. The particles grow to a certain equilibrium size of about 1 mm. The resulting aggregates have a filling factor of about 0.52, assuming a bulk density of 2700 kg m^{-3} for basalt. As seen in Figure 5, the particles are irregularly shaped. For the charge analysis, we approximate the particles as ellipsoids with two small and one large half-axis, which are determined through the video data.

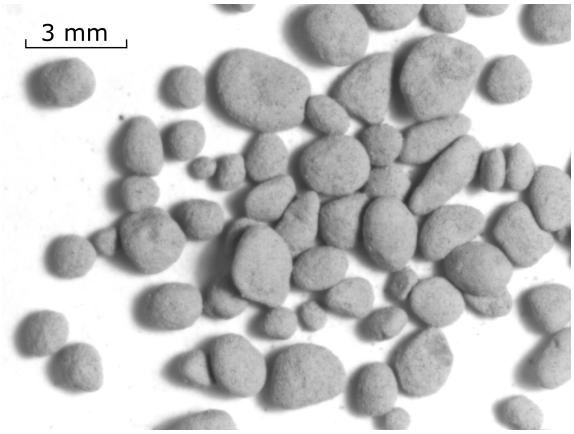

Figure 5. Basalt dust aggregates used as second sample. The particles are irregularly shaped and consist of fine µm-sized grains.

The charge balance for aggregate collisions is depicted in Figure 6. We now see a stronger divergence from a linear distribution and charge conservation as a whole; while for the monolithic beads the data suggest that some charge is lost after impact, we now see charge being lost as well as gained on a much larger scale. In fact, the polarity of a system can even change in some cases. This suggests that there is more at hand than charge being transferred into the gas phase.

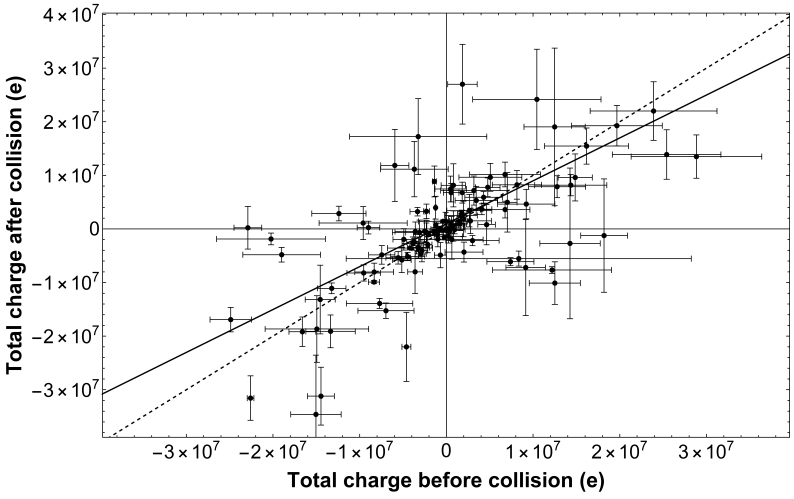

Figure 6. Total charge of two dust aggregates before and after a collision. The solid line is a linear approximation. The dashed line visualizes charge conservation. The individual two-particle systems deviate from charge conservation; charge can be lost as well as gained.

Where we could rule out abrasion before, we now observe small fragments of the aggregates being detached after impact. The collision velocities are not high enough to cause large scale fragmentation, but it is sufficient to detach µm-particles or single dust grains as seen in Figure 7. Assuming that the charge of one particle is distributed over its surface in patches [27], a small fragment could already hold a significant amount of charge. In the following, we further characterize those fragments and the charge they may hold.

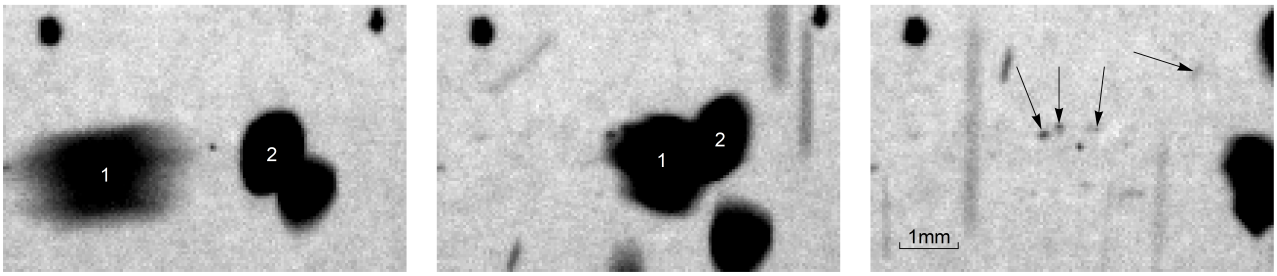

Figure 7. Example of small grains being liberated after two basalt dust aggregates collide. The timeline of the collision event is shown from left to right: before the collision, at the moment of impact and after the collision. The colliding dust aggregates are marked as 1 and 2. The small ejected grains are marked by arrows in the right image.

3.3. Loss of Small Grains

The fragments we see after a collision of two basalt aggregates are on the size scale of a pixel which corresponds to approximately 50 µm. However, their average brightness as seen in the video data is close to the background value, so some of the grains are certainly smaller. We cannot constrain the minimum size with the given optical resolution. However, in view of the recent work by Becker et al. [5], it is likely that particles down to individual micrometer dust grains are ejected. Despite the missing details on the small grain fraction, we can constrain the charge density on these particles to a certain extent.

As a lower charge limit, we deduce values from the accelerations of the smallest particles that we can still trace. These grains are already on the limit of detection. At a certain velocity, particle tracks become unresolved and stretched out, as seen in Figure 7. This reduces the contrast and fast, small grains cannot be traced. The temporal resolution of the video data are limited by a frame rate of 100 fps. This leads to a bias for slow and slowly accelerated, i.e., weakly charged particles. Therefore, we consider the following charge measurements as the lower limit for charges on small grains.

Due to the weak contrast and crowded field of view, the small grains we observe cannot always be attributed to a specific collision of larger aggregates. However, according to Onyeagusi et al. [17], charged grains of pixel size will be accelerated by and eventually stick to one of the electrodes and cannot be ejected or released through recharging. Therefore, we assume that the fine dust that moves freely through the chamber is a result of aggregate collisions and we conclude that its charge is not influenced by recharging at the electrodes.

With the constraints just mentioned, the acceleration of the aggregate fragments is shown in Figure 8 over their normalized brightness B/B_0 with background brightness B_0.

The average brightness of a particle can be determined using Fiji, where the mean grey level of a selected area of an image can be derived. The larger the normalized brightness is, the smaller is the grain. If we assume a geometric absorption of light by grains with a cross-section area A smaller than a pixel, the brightness of this pixel is

$$B = B_0 - B_0 \frac{A}{d_{pix}^2} \tag{2}$$

with square pixels of the size $d_{pix} = 50\,\mu\text{m}$. This translates into a particle diameter of

$$d = \sqrt{1 - \frac{B}{B_0}} d_{pix} \frac{2}{\sqrt{\pi}}. \quad (3)$$

Therefore, the smallest particles with the largest normalized brightness of 0.9 that are still detectable are about d = 18 µm. However, if the particles are not completely opaque, the grains can be larger. This exercise essentially confirms that we cannot resolve grains much smaller than pixel size and we consider d = 50 µm as a reasonable assumption for an average size of the observed small size fraction, noting that there are likely smaller ones, which we simply cannot detect.

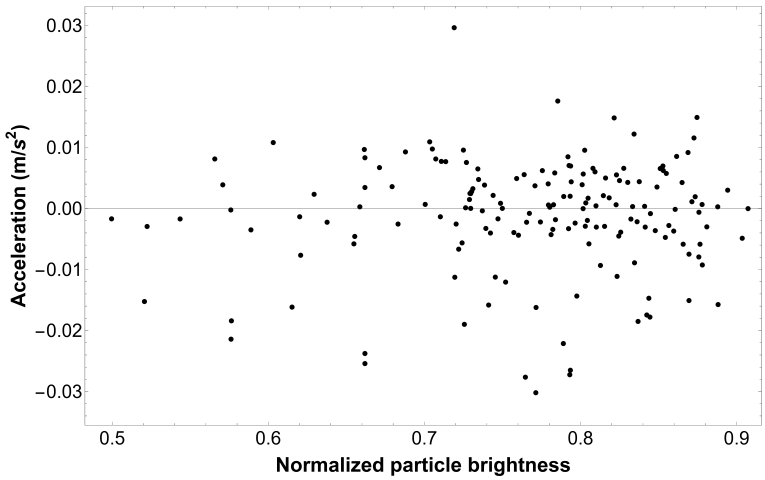

Figure 8. Acceleration of small aggregate fragments over their average brightness value derived from the video data. The brightness values are normalized to the background brightness.

Particles are charged with both polarities. Using the typical acceleration of $a = 0.01\ \mathrm{m/s^2}$ with Equation (1), the small grains would have surface charge densities of at least $\sigma > 1\ \mathrm{nC/m^2}$. We can compare this to the charge density on the original aggregates. Typical charges on an aggregate are $q = 10^7$ e with the elementary charge e $= 1.602 \times 10^{-19}$ C. For a $d = 1$ mm diameter spherical aggregate, this gives a surface charge density of $\sigma \sim 100\ \mathrm{nC/m^2}$.

Therefore, the charge density measured on the small fragments is about two orders of magnitude smaller than on the original aggregate. If all charge is distributed on the surface, a small reduction would be reasonable as the surfaces which are originally within the aggregate would bear no charges. In this case, a reduction by a factor of 100 seems large. If one thinks of an ejected fragment as a cube-like grain with six sides, one of which would be charged, the reduction should be lower than a factor of 10. On the other side, if the charge is not distributed evenly in an aggregate, but occurs as volume charge due to many surfaces between dust grains within the aggregate, ejected grains on the surface could have less charge density. Nonetheless, all this has to be considered in view of a detection bias.

On the upper end, a charge limit on the small grains can be deduced from the charge balance of the collisions. After all, we argue that most of the missing or additional charge after a collision is due to small ejected grains carrying this excess charge. The variation is strong here. As seen in Figure 6, tens of percentages of the absolute charge on both aggregates can be gained or lost. Gaining charge is possible by just shedding small grains of a given surface charge polarity as the two colliding aggregates can have a different polarity. In any case, if the surface charge density was homogeneous, this would imply that, in total, on the order of ∼10% of the surface would be emitted. This is unlikely, even if we cannot detect the very small grains. An ejection of 1 % would be reasonable in view of a 100 µm grain on a 1 mm aggregate. Other explanations would imply local high charge patches that could be emitted [26]. In this case, the charge on a small grain may be up to $1\ \mathrm{\mu C/m^2}$.

In summary, the charge density of a small grain fragment, which was released during the collision of two dust aggregates, may have values of $\sigma = 1\ \mathrm{nC/m^2}$–$1\ \mathrm{\mu C/m^2}$. The lower

limit can be directly measured by tracing the small particles that are still visible in the video data, while the upper limit was derived by the charge balance between the two colliding particles. To further narrow down and specify the charge distribution of those µm-grains, experiments with a higher spatial and temporal resolution are needed.

4. Conclusions

The charge balance on two colliding (sub)-mm sized solid particles shows that some charge "is lost" after the collision. A small fraction may enter into the gas phase of the surrounding atmosphere, but this is not the focus here. More interestingly, dust aggregates also lose charges and they lose a much larger fraction; while these aggregates essentially stay intact at the given small collision velocities well below 1 m/s, small parts can be shed or ejected. Currently, our resolution is limited to grains larger than a few tens of µm. However, we speculate that smaller grains will be ejected as well. In the given setup, these small fragments have at least 1% of the typical charge of the aggregates, but may have up to ten times the average aggregate charge density. This study is but a first indication and the charge and size distributions of the small grains have to be determined in more detail in the future. However, this strongly suggests that, e.g., saltation and charging of large saltating grains will result in charged aerosols in planetary atmospheres.

Author Contributions: Conceptualization and project administration, G.W., J.T. and F.C.O.; methodology, F.C.O.; software and formal analysis, C.M.; validation and writing — original draft preparation, F.C.O. and G.W.; data curation, F.C.O. and C.M.; writing—review and editing, T.B.; visualization, F.C.O., C.M. and G.W.; supervision and funding acquisition, G.W. and J.T. All authors have read and agreed to the published version of the manuscript.

Funding: This project is supported by DLR Space Administration with funds provided by the Federal Ministry for Economic Affairs and Climate Action (BMWK) under grant number DLR 50 WM 2142. T.B. is funded by the European Union's Horizon 2020 research and innovation program under grant agreement No 101004052. The publication of this article was funded by the University of Duisburg-Essen.

Institutional Review Board Statement: Not applicable.

Informed Consent Statement: Not applicable.

Data Availability Statement: Not applicable.

Conflicts of Interest: The authors declare no conflict of interest.

References

1. Greeley, R.; Iversen, J.D. *Wind as a Geological Process on Earth, Mars, Venus and Titan*; Cambridge University Press: New York, NY, USA, 1985. [CrossRef]
2. Tegen, I.; Lacis, A.A. Modeling of particle size distribution and its influence on the radiative properties of mineral dust aerosol. *J. Geophys. Res. Atmos.* **1996**, *101*, 19237–19244. [CrossRef]
3. Lemmon, M.T.; Guzewich, S.D.; McConnochie, T.; de Vicente-Retortillo, A.; Martínez, G.; Smith, M.D.; Bell, J.F.; Wellington, D.; Jacob, S. Large Dust Aerosol Sizes Seen During the 2018 Martian Global Dust Event by the Curiosity Rover. *Geophys. Res. Lett.* **2019**, *46*, 9448–9456. [CrossRef]
4. Chen-Chen, H.; Pérez-Hoyos, S.; Sánchez-Lavega, A. Dust particle size and optical depth on Mars retrieved by the MSL navigation cameras. *Icarus* **2019**, *319*, 43–57. [CrossRef]
5. Becker, T.; Teiser, J.; Jardiel, T.; Peiteado, M.; Muñoz, O.; Martikainen, J.; Martin, J.C.G.; Wurm, G. Releasing Atmospheric Martian Dust in Sand Grain Impacts. *Planet. Sci. J.* **2022**, *3*, 195. [CrossRef]
6. Waza, A.; Kjer, J.; Peiteado, M.; Jardiel, T.; Iversen, J.; Rasmussen, K.; Merrison, J. Aeolian dust resuspension on Mars studied using a recirculating environmental wind tunnel. *Planet. Space Sci.* **2023**, *227*, 105638. [CrossRef]
7. Waitukaitis, S.R.; Lee, V.; Pierson, J.M.; Forman, S.L.; Jaeger, H.M. Size-Dependent Same-Material Tribocharging in Insulating Grains. *Phys. Rev. Lett.* **2014**, *112*, 218001. [CrossRef]
8. Haeberle, J.; Schella, A.; Sperl, M.; Schröter, M.; Born, P. Double origin of stochastic granular tribocharging. *Soft Matter* **2018**, *14*, 4987–4995. [CrossRef]
9. Lacks, D.J.; Shinbrot, T. Long-standing and unresolved issues in triboelectric charging. *Nat. Rev. Chem.* **2019**, *3*, 465–476. [CrossRef]

10. Harrison, R.G.; Barth, E.; Esposito, F.; Merrison, J.; Montmessin, F.; Aplin, K.L.; Borlina, C.; Berthelier, J.J.; Déprez, G.; Farrell, W.M.; et al. Applications of Electrified Dust and Dust Devil Electrodynamics to Martian Atmospheric Electricity. *Space Sci. Rev.* **2016**, *203*, 299–345. [CrossRef]
11. Cimarelli, C.; Alatorre-Ibarguengoitia, M.A.; Kueppers, U.; Scheu, B.; Dingwell, D.B. Experimental generation of volcanic lightning. *Geology* **2014**, *42*, 79–82. [CrossRef]
12. Schmidt, D.S.; Schmidt, R.A.; Dent, J.D. Electrostatic force on saltating sand. *J. Geophys. Res. Atmos.* **1998**, *103*, 8997–9001. [CrossRef]
13. Zheng, X.J.; Huang, N.; Zhou, Y.H. Laboratory measurement of electrification of wind-blown sands and simulation of its effect on sand saltation movement. *J. Geophys. Res. (Atmos.)* **2003**, *108*, 4322. [CrossRef]
14. Zhang, H.; Zheng, X.J.; Bo, T. Electrification of saltating particles in wind-blown sand: Experiment and theory. *J. Geophys. Res. (Atmos.)* **2013**, *118*, 12086–12093. [CrossRef]
15. Kok, J.F.; Renno, N.O. Enhancement of the emission of mineral dust aerosols by electric forces. *Geophys. Res. Lett.* **2006**, *33*, L19S10. [CrossRef]
16. Esposito, F.; Molinaro, R.; Popa, C.I.; Molfese, C.; Cozzolino, F.; Marty, L.; Taj-Eddine, K.; Di Achille, G.; Franzese, G.; Silvestro, S.; et al. The role of the atmospheric electric field in the dust-lifting process. *Geophys. Res. Lett.* **2016**, *43*, 5501–5508. [CrossRef]
17. Onyeagusi, F.C.; Jungmann, F.; Teiser, J.; Wurm, G. Electrostatic Repulsion of Dust from Planetary Surfaces. *Planet. Sci. J.* **2023**, *4*, 13. [CrossRef]
18. Matsuyama, T. A discussion on maximum charge held by a single particle due to gas discharge limitation. In Proceedings of the 1st International Conference and Exhibition on Powder Technology Indonesia (ICePTi) 2017, Jatinangor, Indonesia, 8–9 August 2017; American Institute of Physics Conference Series; 2018; Volume 1927, p. 020001. [CrossRef]
19. Wurm, G.; Schmidt, L.; Steinpilz, T.; Boden, L.; Teiser, J. A challenge for Martian lightning: Limits of collisional charging at low pressure. *Icarus* **2019**, *331*, 103–109. [CrossRef]
20. Schoenau, L.; Steinpilz, T.; Teiser, J.; Wurm, G. Corona discharge of a vibrated insulating box with granular medium. *Granul. Matter* **2021**, *23*, 1–6. [CrossRef]
21. Jungmann, F.; van Unen, H.; Teiser, J.; Wurm, G. Violation of triboelectric charge conservation on colliding particles. *Phys. Rev. E* **2021**, *104*, L022601. [CrossRef]
22. Schindelin, J.; Arganda-Carreras, I.; Frise, E.; Kaynig, V.; Longair, M.; Pietzsch, T.; Preibisch, S.; Rueden, C.; Saalfeld, S.; Schmid, B.; et al. Fiji: an open-source platform for biological-image analysis. *Nat. Methods* **2012**, *9*, 676–682. [CrossRef]
23. McCarty, L.S.; Winkleman, A.; Whitesides, G.M. Ionic Electrets: Electrostatic Charging of Surfaces by Transferring Mobile Ions upon Contact. *J. Am. Chem. Soc.* **2007**, *129*, 4075–4088. [CrossRef]
24. Lee, V.; James, N.M.; Waitukaitis, S.R.; Jaeger, H.M. Collisional charging of individual submillimeter particles: Using ultrasonic levitation to initiate and track charge transfer. *Phys. Rev. Mater.* **2018**, *2*, 035602. [CrossRef]
25. Harris, I.A.; Lim, M.X.; Jaeger, H.M. Temperature dependence of nylon and PTFE triboelectrification. *Phys. Rev. Mater.* **2019**, *3*, 085603. [CrossRef]
26. Jungmann, F.; Onyeagusi, F.C.; Teiser, J.; Wurm, G. Charge transfer of pre-charged dielectric grains impacting electrodes in strong electric fields. *J. Electrost.* **2022**, *117*, 103705. [CrossRef]
27. Steinpilz, T.; Jungmann, F.; Joeris, K.; Teiser, J.; Wurm, G. Measurements of dipole moments and a Q-patch model of collisionally charged grains. *New J. Phys.* **2020**, *22*, 093025. [CrossRef]

DOI: 10.3390/atmos14071065
URN: urn:nbn:de:hbz:465-20230901-151436-2